Egypt. J. Chem. **Vol. 67**, No. 11 pp. 83 - 97 (2024)

Egyptian Journal of Chemistry

http://ejchem.journals.ekb.eg/

Facile Synthesis, *In silico* Studies, and Biological Assessment of Novel Pyrazolo[3,4-*b*]pyridine Congeners

Ibrahim F. Nassar[a,*], Adel A.-H. Abdel Rahman[b], Esraa M. Elnemr[b], Mohamed A. Said[c], Mohamed G. Abouelenein[b]

[*a]*Faculty of Specific Education, Ain Shams University, 365- Ramsis stret, Abassia, Cairo, Egypt*
[b]*Chemistry Department, Faculty of Science, Menoufia University, Shebin El-Kom, Egypt.*
[c]*Pharmaceutical Chemistry department, Faculty of Pharmacy, Egyptian Russian University, Badr City, Cairo, 11829, Egypt*

Abstract

The present work depicts synthesizing an innovative sequence of polyfunctionalized Pyrazolo[3,4-*b*]pyridine congeners **2-12** and assessed for antimicrobial, antitumor, telomerase inhibition, and anti-hepatitis B efficacies applying an array of techniques. Fortunately, most of the compounds demonstrated auspicious bio efficiencies. Additionally, *in silico* simulation was executed for determining the synthetic Pyrazolo[3,4-*b*]pyridines anticipated mode of action. Compounds **4**, **5**, and **6** were picked as the most potent and efficient candidates versus the telomerase enzyme [PDB id: 2B2A]. The consequences exposed that compound **5** is the extremely credible operative in contradiction of telomerase enzyme as it disclosed the best binding score and interaction pose. These initial outcomes may improve in introducing more research strategies converged on pyrazolo[3,4-*b*]pyridines, exclusively those with anticipated bioefficacy, ultimate ADMET parameters, and constructive prospects.

Keywords: Pyrazolo[3,4-*b*]pyridine, Telomerase, Molecular docking, Pyridine, ADMET, Antitumor, Antimicrobial, Anti-hepatitis B.

1. Introduction

Nitrogen-comprising heterocycles are very influential frameworks for discovering compelling bioactive agents in agrochemicals and pharmaceuticals [1–4]. Amongst these heterocyclic systems, exclusively those encompassing pyridine ring are correlated with varied pharmacologic possessions like antimicrobial [5], anticancer [6], antiviral [7], anticonvulsant [8], antifungal [9], and anti-HIV efficacies [10]. The pyrazolo[3,4-*b*]pyridine scaffold is a crucial structural segment of numerous heterocyclic scaffolds, playing a crucial role in agrochemical and pharmacological research [11].

Pyrazolo[3,4-*b*]pyridine scaffolds acquired significant attention in medicinal chemistry for their potent and privileged range of biological efficacies as applied with GSK-3 inhibition [12], antibacterial [13], anticancer [14], antiviral [15], antifungal [16], antitumor [17], antileishmanial [18], cyclin-dependent kinases inhibition [19], antiproliferative [20], anxiolytic [21], anti-inflammatory [22], cardiovascular [23], anti-Alzheimer [24], antimicrobial [25], and antimalarial efficiencies [26]. They were also applied as adenosine antagonists [27], bone metabolism improvers [28], controlling herbicides [29], and blood platelet aggregation

*Corresponding author e-mail: dr.ibrahim.nassar@sedu.asu.edu.eg.; (Ibrahim F. Nassar).
EJCHEM use only: Received date 05 April 2024; revised date 24 April 2024; accepted date 07 May 2024
DOI: 10.21608/ejchem.2024.280985.9546

inhibitors [30]. Investigation of marketed drugs encompassing 1*H*-Pyrazolo[3,4-*b*]pyridines has been illuminated due to their distinct impacts in various scopes. A group of anxiolytic-antidepressant drugs from this scaffold; Tracazolate, Etazolate, cartazolate, LASSBio-981, LASSBio-873, LASSBio-872, and LASSBio-982 have been used to treat anxiety disorder related with GABA induced neuroinhibition (Figure 1) [31]. Several synthetic approaches have been employed for synthesizing pyrazolopyridines under diverse conditions [32, 33].

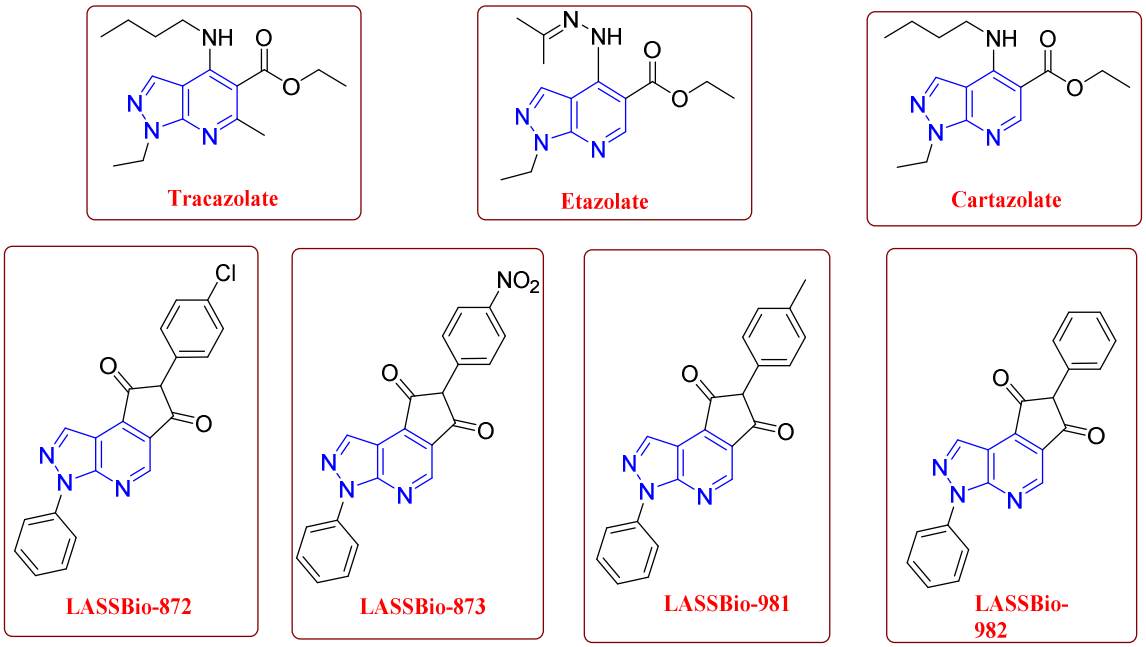

Figure 1. Drugs comprising Pyrazolo[3,4-*b*]pyridine scaffold.

Boosted by the beforehand statements, encompassing our achievements to inquest specific Pyrazolo[3,4-*b*]pyridine congeners imperilling anticipated bio efficiency was worthwhile. In our contemporary work, an innovative succession of pyrazolo[3,4-*b*]pyridines was synthesized and assessed for their antimicrobial, antitumor, telomerase inhibition, and anti-hepatitis B efficacies applying an array of techniques. Over and above, *in silico* studies were executed for determining the expected mode of action of the synthetic Pyrazolo[3,4-*b*]pyridines.

2. Experimental section

2.1 Chemistry

Employing a *Kofler* block apparatus, melting points were uncovered and uncorrected. Utilizing KBr disks, the IR spectra were documented on a Thermo Fisher Scientific FTIR spectrometer (cm^{-1}). ^{1}H, ^{13}C NMR spectra were recorded on a JEOL spectrometer (500, 100 MHz) employing TMS (δ) as the internal standard and DMSO-d_6 as a solvent. Applying a Shimadzu Gas chromatography instrument mass spectrometer (70 eV), Mass spectra were obtained. Utilizing aluminum silica gel plates 60 F245, the reactions' progress was monitored *via* TLC. At the National Cancer Institute (NCI), Cairo, Egypt, the synthesized compounds' anticancer efficacy was executed. At the Liver Institute, Shebin El-Kom Egypt, the antiviral efficiency versus HBV was tested.

*2.1.1 4-(2-methoxybenzylidene)-5-methyl-2-phenyl-2,4-dihydro-3H-pyrazol-3-one (**1**)*

To an ethanolic solution (30 mL) of 3-methyl-1-phenyl-1*H*-pyrazol-5(4*H*)-one (1.74 g,10 mmol), 2-methoxybenzaldehyde (1.2 mL, 10 mmol) and NaOH (20%, 15 mL) were added portion-wise with stirring for 4 h. The mix was poured over icy water and then neutralized with dil. HCl. The resulting precipitate was filtered off, dried, and recrystallized from ethanol furnishing compound **1** as orange crystals. Yield 78%; mp: 200-202 °C; IR (KBr) $cm^{-1}\nu_{max}$: 3064, 2919, 1686, 1597, 1575, 1464; ^{1}H NMR (500 MHz, DMSO-d_6) δ (ppm): 8.01 (s, 1H, CH=C), 6.94-7.99 (m, 9H, Ar-H), 3.9 (s, 3H, OCH_3), 2.33 (s, 3H); ^{13}C

NMR (100 MHz, DMSO-d_6) δ (ppm): 164.12, 159.64, 147.92, 143.35, 141.06, 134.87, 130.12 (2C), 129.57, 128.36, 124.76, 122.27, 119.21 (2C), 118.04, 115.09, 57.46, 15.96; EIMS, *m/z* $[M]^+$ calcd: 292.34; found: 292.12; Elemental Analysis for $C_{18}H_{16}N_2O_2$ (%), Calcd: C, 73.95; H, 5.52; N, 9.58; found: C, 73.88; H, 5.57; N, 9.65.

*4-(2-methoxyphenyl)-3-methyl-6-oxo-1-phenyl-6,7-dihydro-1H-pyrazolo[3,4-b]pyridine-5-carbonitrile (**2**)*

Method A: To a solution of compound **1** (2.9 g, 10 mmol) in absolute EtOH (30 mL), ammonium acetate (0.77 g, 10 mmol), and ethyl cyanoacetate (1.06 mL, 10 mmol) were added and refluxed for 10 h and then cooled. After the reaction mixture's concentration, the residue was recrystallized from MeOH, affording compound **2** as a golden powder.

Method B: A mix of 3-methyl-1-phenyl-1*H*-pyrazol-5(4*H*)-one (1.74 g, 10 mmol), 2-methoxybenzaldehyde (1.2 mL, 10 mmol), ammonium acetate (0.77 g, 10 mmol), and ethyl cyanoacetate (1.06 mL, 10 mmol) was irradiated in microwave (power 270 W) for 6 min. After cooling, the detached solid was filtered off, washed with EtOH, desiccated, and recrystallized from EtOH, allowing compound **2** as a golden powder. Yield 90%; mp: 240-242°C; IR (KBr) $cm^{-1}\nu_{max}$: 3354, 3087, 2934, 2839, 2205, 1645, 1623, 1591; ^{1}H NMR (500 MHz, DMSO-d_6) δ (ppm): 11.12 (br.s, 1H, NH), 6.95-7.98 (m, 9H, Ar-H), 3.87 (s, 3H, -OCH_3), 2.38 (s, 3H); ^{13}C NMR (100 MHz, DMSO-d_6) δ (ppm): 168.25, 165.23, 158.31, 147.94, 140.36, 139.78, 131.74 (2C), 129.24, 128.53, 126.13 (2C), 123.84, 121.07, 117.08 (CN), 113.19, 111.89, 102.76, 98.02, 57.46, 15.96; EIMS, *m/z* $[M]^+$ calcd: 356.39; found: 356.13; Elemental Analysis for $C_{21}H_{16}N_4O_2$ (%), Calcd: C, 70.77; H, 4.53; N, 15.72; found: C, 70.69; H, 4.49; N, 15.67.

*Ethyl 2-((5-cyano-4-(2-methoxyphenyl)-3-methyl-1-phenyl-1H-pyrazolo[3,4-b]pyridin-6-yl)oxy)acetate (**3**)*

To a mix of pyrazolo[3,4-*b*]pyridine-5-carbonitrile **2** (3.56 g, 10 mmol) and potassium carbonate (12 mmol) in DMF (15 mL), ethyl chloroacetate (1.22 mL, 10 mmol) was added and stirred for 12 h. The precipitant was filtered, and the filtrate was poured over ice-cold water. The obtained precipitate was filtered off, dried up, and recrystallized from ethyl alcohol, furnishing **3** as a yellow powder. Yield 65%; mp: 250-252 °C; IR (KBr) $cm^{-1}\nu_{max}$: 3054, 2934, 2839, 2200, 1732, 1635, 1612, 1591; ^{1}H NMR (500 MHz, DMSO-d_6) δ (ppm): 7.01-8.04 (m, 9H, Ar-H), 4.62 (s, 2H, O**CH$_2$**), 4.12-4.16 (q, 2H, COO**CH$_2$**), 3.79 (s, 3H, OCH_3), 2.39 (s, 3H, CH_3), 1.22-1.26 (t, 3H, CH_3); ^{13}C NMR (100 MHz, DMSO-d_6) δ (ppm): 170.05, 167.34, 158.41, 154.23, 151.78, 146.12, 141.03, 131.24 (2C), 129.24 (2C), 128.51, 126.28, 122.84, 120.06 (2C), 117.14, 115.24 (CN), 113.19, 99.02, 64.01, 61.94, 57.85, 13.45, 11.27; EIMS, *m/z* $[M]^+$ calcd: 442.48; found: 442.95; Elemental Analysis for $C_{25}H_{22}N_4O_4$ (%), Calcd: C, 67.86; H, 5.01; N, 12.66; found: C, 67.81; H, 4.95; N, 12.62.

*2-((5-cyano-4-(2-methoxyphenyl)-3-methyl-1-phenyl-1H-pyrazolo[3,4-b]pyridin-6-yl)oxy)acetohydrazide (**4**)*

To the ethyl ester congener **3** ethanolic solution (4.4 g, 10 mmol) (30 mL), hydrazine hydrate (2 mL, 15 mmol) was added. The mix was refluxed for 6 h then cooled. The resulting solid was filtered off and recrystallized from aqueous EtOH, giving **4** as a brown powder. Yield: 70%; mp: 240-246 °C; IR (KBR) $cm^{-1}\nu_{max}$: 3319, 3245, 3132, 3065, 3000, 2924, 2841, 2201, 1656, 1612, 1599; ^{1}H NMR (500 MHz, DMSO-d_6) δ (ppm): 9.87 (br.s, 1H, NH), 7.02-8.05 (m, 9H, Ar-H), 4.59 (s, 2H, CH_2), 4.31 (s, 2H, NH_2), 3.79 (s, 3H, OCH_3), 2.09 (s, 3H, CH_3); ^{13}C NMR (100 MHz, DMSO-d_6) δ (ppm): 168.84, 166.04, 157.76, 153.95, 151.01, 145.74, 140.49, 131.07 (2C), 129 (2C), 127.86, 125.76, 122.08, 119.87 (2C), 116.74, 115.17 (CN), 112.56, 98.64, 67.59, 57.12, 13.12; EIMS, *m/z* $[M]^+$ calcd: 428.45; found: 428.99; Elemental Analysis for $C_{23}H_{20}N_6O_3$ (%), Calcd: C, 64.48; H, 4.71; N, 19.62; found: C, 64.42; H, 4.65; N, 19.58.

*2-((5-cyano-4-(2-methoxyphenyl)-3-methyl-1-phenyl-1H-pyrazolo[3,4-b]pyridin-6-yl)oxy)-N′-((2S,3R,4R,5R,E)-2,3,4,5,6-pentahydroxyhexylidene)acetohydrazide (**5**)*

To an ethanolic solution of compound **4** (2.14 g, 5 mmol) (30 mL), D-glucose (1g, 5 mmol) and glacial AcOH drops were added and refluxed for 7 h then cooled. The precipitate was filtered off, dried up, and recrystallized from MeOH, affording **5** as a brown powder. Yield: 75%; mp: 208-210 °C; IR (KBr) $cm^{-1}\nu_{max}$: 3365, 3145, 2917, 2850, 2208, 1648, 1634, 1601, 1595; ^{1}H NMR (500 MHz, DMSO-d_6) δ (ppm): 9.91 (br.s, 1H, NH), 8.26-8.274 (d, 1H, *J*= 7 Hz), 7.03-8.06 (m, 9H, Ar-H), 5.64-5.654 (d, 1H, *J*= 7 Hz), 5.25-5.26 (m, 2H), 4.61 (s, 2H, CH_2), 4.42-4.44 (m, 2H), 3.79 (s, 3H, OCH_3), 3.67-3.684 (d, 1H,

J= 7 Hz), 3.61-3.62 (m, 2H), 3.44-3.454 (t, 1H, *J*= 7 Hz), 3.30-3.31 (m, 2H), 2.11 (s, 3H, CH_3); ^{13}C NMR (100 MHz, DMSO-d_6) δ (ppm): 170.53, 167.13, 158.78, 157.24, 154.43, 152.14, 146.19, 141.51, 131.68 (2C), 130.17 (2C), 128.21, 126.09, 123.06, 120.25 (2C), 117.29, 116.31 (CN), 113.96, 99.71, 73.83, 71.61, 70, 67.21, 66.36, 63.84, 57.39, 13.27; EIMS, *m/z* $[M]^+$ calcd: 590.59; found: 591.42; Elemental Analysis for $C_{29}H_{30}N_6O_8$ (%), Calcd: C, 58.98; H, 5.12; N, 14.23; found: C, 58.9; H, 5.19; N, 14.18.

*2-((5-cyano-4-(2-methoxyphenyl)-3-methyl-1-phenyl-1H-pyrazolo[3,4-b]pyridin-6-yl)oxy)-N′-((2R,3S,4S,E)-2,3,4,5-tetrahydroxypentylidene)acetohydrazide (**6**)*

To an ethanolic solution of compound **4** (2.14 g, 5 mmol) (30 mL), D-xylose (1 g, 5 mmol) and glacial AcOH drops were added and refluxed for 6 h and then cooled. The precipitate was filtered off, dried up, and recrystallized from MeOH, affording **6** as a brown powder. Yield: 65%; mp 206-208 °C; IR (KBr) $cm^{-1}\nu_{max}$: 3353, 3156, 2924, 2862, 2203, 1649, 1633, 1605, 1598; ^{1}H NMR (500 MHz, DMSO-d_6) δ (ppm): 9.86 (br.s, 1H, NH), 8.2-8.216 (d, 1H, *J*= 8 Hz), 7-8.03 (m, 9H, Ar-H), 5.3-5.31 (m, 2H), 4.95-5.96 (m, 2H), 4.58 (s, 2H, CH_2), 4.36-4.38 (m, 1H), 3.78 (s, 3H, OCH_3), 3.75-3.76 (m, 2H), 3.59-3.60 (m, 2H), 2.1 (s, 3H, CH_3); ^{13}C NMR (100 MHz, DMSO-d_6) δ (ppm): 170.12, 166.79, 158.14, 157.06, 154.14, 152.01, 145.91, 141.24, 131.15 (2C), 130.09 (2C), 128.03, 126.01, 122.84, 120.14 (2C), 117.07, 115.94 (CN), 112.27, 99.29, 73.91, 71.69, 67.46, 66.12, 64.26, 57.09, 13.37; EIMS, *m/z* $[M]^+$ calcd: 560.57; found: 559.05; Elemental Analysis for $C_{28}H_{28}N_6O_7$ (%), Calcd: C, 59.99; H, 5.03; N, 14.99; found: C, 59.91; H, 5.11; N, 14.92.

*(1R,2S,3R,4R)-1-(3-acetyl-5-(((5-cyano-4-(2-methoxyphenyl)-3-methyl-1-phenyl-1H-pyrazolo[3,4-b]pyridin-6-yl)oxy)methyl)-2,3-dihydro-1,3,4-oxadiazol-2-yl)pentane-1,2,3,4,5-pentayl pentaacetate (**7**)*

To an ethanolic solution of compound **5** (5.9 g, 10 mmol) (25 mL), acetic anhydride (15 mL) was appended and refluxed for 3 h. The resulting solution was concentrated and cooled. The precipitate was filtered off, dried up, and recrystallized from MeOH, giving **7** as a dark brown powder. Yield: 78%; mp: 202-204 °C; IR (KBr) $cm^{-1}\nu_{max}$: 3065, 2924, 2862, 2203, 1738, 1631, 1600, 1594; ^{1}H NMR (500 MHz, DMSO-d_6) δ (ppm): 1.96, 1.97, 2.02, 2.05, 2.08 (6s, 18H, 6 OAc), 2.23 (s, 3H, CH_3 (pyrazole)), 3.80 (s, 3H, OCH_3), 4.09-4.15 (m, 2H, $H^{6'}$), 4.22 (m, 1H, $H^{5'}$), 4.64 (s, 2H, CH_2), 5.15 (t, 1H, $J^{3',4'}$= 15.8 Hz, $H^{4'}$), 5.25 (t, 1H, $J^{2',3'}$= 15.3 Hz, $H^{2'}$), 5.67 (t, 1H, $J^{2',3'}$=15.8 Hz, $H^{3'}$), 6.51 (d, 1H, $J^{1',2'}$= 13.6 Hz, $H^{1'}$), 6.76-8.30 (m, 9H, Ar-H); ^{13}C NMR (100 MHz, DMSO-d_6) δ (ppm): 171.92, 171.67, 170.89, 170.76, 170.53, 168.49, 167.19, 158.83, 157.29, 152.18, 146.26, 141.6, 131.72 (2C), 130.19 (2C), 128.32, 126.14, 123.13, 120.29 (2C), 117.54, 116.46 (CN), 114.03, 99.86, 78.31, 77.61, 73.14, 71.01, 67.45, 66.41, 62.09, 61.23, 57.43, 23.46, 22.12, 21.07, 20.64, 18.35, 17.91, 13.34; EIMS, *m/z* $[M]^+$ calcd: 842.82; found: 841.78; Elemental Analysis for $C_{41}H_{42}N_6O_{14}$ (%), Calcd: C, 58.43; H, 5.02; N, 9.97; found: C, 58.37; H, 5.09; N, 9.94.

*(1R,2S,3R)-1-(3-acetyl-5-(((5-cyano-4-(2-methoxyphenyl)-3-methyl-1-phenyl-1H-pyrazolo[3,4-b]pyridin-6-yl)oxy)methyl)-2,3-dihydro-1,3,4-oxadiazol-2-yl)butane-1,2,3,4-tetrayltetraacetate (**8**)*

To an ethanolic solution of compound **6** (5.9 g, 10 mmol) (25 mL), acetic anhydride (15 mL) was added and refluxed for 6 h. The mix was concentrated and iced. The precipitate was filtered off, dried up, and recrystallized from MeOH, affording **8** as a dark brown powder. Yield: 78%; mp: 202-204°C; IR (KBr) $cm^{-1}\nu_{max}$: 3056, 2934, 2865, 2214, 1739, 1630, 1601, 1593; ^{1}H NMR (500 MHz, DMSO-d_6) δ (ppm): 1.97, 1.98, 2.03, 2.06, 2.08 (5s, 15H, 5 OAc), 2.24 (s, 3H, CH_3 (pyrazole)), 3.79 (s, 3H, OCH_3), 4.10-4.16 (m, 2H, $H^{5'}$), 4.68 (s, 2H, CH_2), 4.79 (m, 1H, $H^{4'}$), 5.37 (t, 1H, $J^{2',3'}$= 15.3 Hz, $H^{3'}$), 5.69 (t, 1H, $J^{2',3'}$=15.8 Hz, $H^{2'}$), 6.49 (d, 1H, $J^{1',2'}$= 13.6 Hz, $H^{1'}$), 6.78-8.32 (m, 9H, Ar-H); ^{13}C NMR (100 MHz, DMSO-d_6) δ (ppm): 171.74, 170.91, 170.74, 170.56, 168.51, 167.19, 158.71, 157.23, 152.12, 150.23, 146.22, 141.58, 131.71 (2C), 130.15 (2C), 128.30, 126.11, 123.11, 120.26 (2C), 117.50, 116.42 (CN), 114.01, 99.83, 76.59, 75.06, 72.09, 67.49, 65.45, 61.14, 57.31, 23.39, 22.11, 21.04, 20.54, 18.25, 13.36; EIMS, *m/z* $[M]^+$ calcd: 770.75; found: 771.45; Elemental Analysis for $C_{38}H_{38}N_6O_{12}$ (%), Calcd: C, 59.22; H, 4.97; N, 10.9; found: C, 59.18; H, 4.92; N, 10.96.

*N′-(4-chlorobenzylidene)-2-((5-cyano-4-(2-methoxyphenyl)-3-methyl-1-phenyl-1H-pyrazolo[3,4-b]pyridin-6-yl)oxy)acetohydrazide (**9**)*

To an ethanolic solution of compound **4** (2.14 g, 5 mmol) (30 mL), 4-chlorobenzaldehyde (0.7g, 5 mmol) and glacial AcOH drops were supplemented, then refluxed for 5 h and iced. The attained precipitate was filtered off, dried up, and recrystallized from MeOH, furnishing **9** as a yellow powder. Yield: 85%; mp: 219-221 °C; IR (KBr) $cm^{-1}\nu_{max}$: 3213, 3034, 2934, 2865, 2224, 1649, 1614, 1599; ^{1}H NMR (500 MHz, DMSO-d_6) δ (ppm): 11.07 (br.s, 1H, NH), 8.58 (s, 1H, CH=*N*), 7.1-8.34 (m, 13H, Ar-H), 4.63 (s, 2H, CH_2), 3.84 (s, 3H, OCH_3), 2.12 (s, 3H, CH_3); ^{13}C NMR (100 MHz, DMSO-d_6) δ (ppm): 170.99, 165.64, 158.23, 154.17, 152.18, 150.99, 144.71 (2C), 139.18, 136.18, 130.73 (2C), 129.14 (2C), 128.53 (2C), 127.98, 123.91, 122.14, 119.92 (2C), 116.43, 115.86 (CN), 113.83, 112.15 (2C), 98.23, 67.84, 56.81, 13.57; EIMS, *m/z* $[M]^+$ calcd: 551.15; found: 551.13; Elemental Analysis for $C_{30}H_{23}ClN_6O_3$ (%), Calcd: C, 65.4; H, 4.21; N, 15.25; found: C, 65.34; H, 4.16; N, 15.28.

*6-((4-acetyl-5-(4-chlorophenyl)-4,5-dihydro-1,3,4-oxadiazol-2-yl)methoxy)-4-(2-methoxyphenyl)-3-methyl-1-phenyl-1H-pyrazolo[3,4-b]pyridine-5-carbonitrile (**10**)*

To an ethanolic solution of compound **9** (5.51g, 10 mmol (25 mL), acetic anhydride (15 mL) was supplemented and refluxed for 4 h. The subsequent mix was concentrated and cooled. The acquired mass was filtered off, dried up, and recrystallized from EtOH, affording **10** as a brown powder. Yield: 78%; mp: 202-204°C; IR (KBr) $cm^{-1}\nu_{max}$: 3078, 2954, 2886, 2224, 1655, 1639, 1604, 1590; ^{1}H NMR (500 MHz, DMSO-d_6) δ (ppm): 6.71-8.24 (m, 14H, Ar-H), 4.73 (s, 2H, CH_2), 3.83 (s, 3H, OCH_3), 2.22 (s, 3H, CO**CH$_3$**), 2.1 (s, 3H, CH_3); ^{13}C NMR (100 MHz, DMSO-*d6*) δ (ppm): 169.12, 165.23, 158.31, 154.32, 152.42, 150.99, 149.67, 144.39, 139.37, 138.24, 132.19, 130.51 (2C), 129.92, 129.31 (2C), 127.99 (2C), 127.06, 126.19, 121.82, 119.93 (2C), 116.53, 115.72 (CN), 113.92, 98.46, 84.62, 71.08, 56.95, 21.12, 13.61; EIMS, *m/z* $[M]^+$ calcd: 593.04; found: 593.74; Elemental Analysis for $C_{32}H_{25}ClN_6O_4$ (%), Calcd: C, 64.81; H, 4.25; N, 14.17; found: C, 64.78; H, 4.29; N, 14.23.

*2-((5-cyano-4-(2-methoxyphenyl)-3-methyl-1-phenyl-1H-pyrazolo[3,4-b]pyridin-6-yl)oxy)-N′-(4-(dimethylamino)benzylidene)acetohydrazide (**11**)*

To an ethanolic solution of compound **4** (2.14 g, 5 mmol) (30 mL), *p*-dimethylaminobenzaldehyde (0.74 g, 5 mmol) and drops of glacial AcOH were supplemented and refluxed for 5 h and then cooled. The attained dense was filtered off, desiccated, and recrystallized from EtOH, giving **11** as an orange powder. Yield: 65%; mp: 230-232 °C; IR (KBr) $cm^{-1}\nu_{max}$: 3204, 3029, 2929, 2862, 2220, 1648, 1609, 1598; ^{1}H NMR (500 MHz, DMSO-d_6) δ (ppm): 11.04 (br.s, 1H, NH), 8.43 (s, 1H, CH=*N*), 7.08-8.32 (m, 13H, Ar-H), 4.61 (s, 2H, CH_2), 3.81 (s, 3H, OCH_3), 3.04 (s, 6H, $N(CH_3)_2$), 2.1 (s, 3H, CH_3); ^{13}C NMR (100 MHz, DMSO-d_6) δ (ppm): 170.94, 165.23, 158.11, 154.01, 152.07, 150.97, 144.62 (2C), 139.07, 130.62 (2C), 129.08 (2C), 128.46 (2C), 127.96, 126.09, 123.86, 122.08, 119.87 (2C), 116.39, 115.71 (CN), 113.76, 112.09 (2C), 98.13, 67.76, 56.79, 40.97 (2C), 13.47; EIMS, *m/z* $[M]^+$ calcd: 559.23; found: 559.39; Elemental Analysis for $C_{32}H_{29}N_7O_3$ (%), Calcd: C, 68.68; H, 5.22; N, 17.52; found: C, 68.62; H, 5.18; N, 17.47.

*6-((4-acetyl-5-(4-(dimethylamino)phenyl)-4,5-dihydro-1,3,4-oxadiazol-2-yl)methoxy)-4-(2-methoxyphenyl)-3-methyl-1-phenyl-1H-pyrazolo[3,4-b]pyridine-5-carbonitrile (**12**)*

To an ethanolic solution of compound **11** (5.59 g, 10 mmol) (25 mL), acetic anhydride (15 mL) was supplemented and refluxed for 4 h. The subsequent mix was concentrated and cooled. The acquired solid was filtered, dried up, and recrystallized from EtOH, furnishing compound **12** as a brown powder. Yield: 78%; mp: 202-204°C; IR (KBr) $cm^{-1}\nu_{max}$: 3075, 2949, 2881, 2219, 1656, 1638, 1602, 1591; ^{1}H NMR (400 MHz, DMSO-*d*6) δ (ppm): 6.69-8.25 (m, 14H, Ar-H), 4.72 (s, 2H, CH_2), 3.82 (s, 3H, OCH_3), 3.05 (s, 6H, $N(CH_3)_2$), 2.2 (s, 3H, CO**CH$_3$**), 2.09 (s, 3H, CH_3); ^{13}C NMR (100 MHz, DMSO-*d*6) δ (ppm): 169.13, 165.19, 158.29, 154.25, 152.32, 150.98, 149.41, 144.23, 139.17, 130.45 (2C), 129.89, 129.21 (2C), 127.97 (2C), 127.04, 126.13, 121.78, 119.88 (2C), 116.45, 115.64 (CN), 113.86, 112.16 (2C), 98.24, 84.51, 70.41, 56.87, 41.02 (2C), 21.08, 13.50; EIMS, *m/z* $[M]^+$ calcd: 601.67; found: 601.88; Elemental Analysis for $C_{34}H_{31}N_7O_4$ (%), Calcd: C, 67.87; H, 5.19; N, 16.3; found: C, 67.83; H, 5.15; N, 16.26.

2.2 Antimicrobial assessment

Designed for the screening approach, the Cruickshank *et al* [34] agar diffusion method was applied. On Czapek's-Dox agar media and nutrient agar, the fungi as well as bacteria were retained, correspondingly. The assay medium hipflasks

comprehending 50 mL Czapek's-Dox agar medium (fungi) and nutrient agar (bacteria) correspondingly were certified to accomplish 40-50 ^{o}C for inoculating with 0.5 mL test organism cell suspension. Afterward flawless shuffling, every hipflask was poured over a Petri dish (15 x 2 cm) and authorized for solidifying. Utilizing a sterile cork poorer (diameter 6 mm), holes (0.6 cm diameter) were accomplished, afterwards hardening in the agar plate. In 2 mL DMSO, every synthetic pyrazolo[3,4-*b*]pyridine was thawed. Employing a micropipette, every synthetic pyrazolo[3,4-*b*]pyridine (100µl) was positioned in these hollows. For 1 h at 5 °C, the Petri dishes were succumbed in favor of warranting the agar medium-samples diffusion and hindering the testified organism growing. Plates incubation was set for 72 h at 28 ^{o}C (fungi) and for 24 h at 30 ^{o}C (bacteria). DMSO exhibited certainly not inhibition zones. The inhibition zone diameters were assessed linking with the indication (penicillin (50 µg/mL)), the outcomes were formulated, and the commented inhibition zones were exposed (Table 1).

2.3 In vitro Antitumor Efficiency

2.3.1 Potential Cytotoxicity Measurement Employing SRB assay.

Utilizing Storeng and Skehan approach, the pyrazolo[3,4-*b*]pyridine congeners **1-12** were assessed for their Cytotoxicity in contradiction of breast cancer (**MCF-7**) [35]. In 96-multiwell plate (10^4 cells / well), Cells were sheeted beforehand the compounds treatment for 24 h for allowing the cell-plate wall connection. For every single dose, the testified compound dissimilar concentrations (0, 1, 2.5, 5, and 10 µg/ml) were equipped and supplemented to the cell monolayer triplicate wells. For 48 h, monolayer cells were incubated at 37 °C + 5 % CO_2 with the pyrazolo[3,4-*b*]pyridines **1-12**. Cells were restored, washed, and tainted with Sulfo-Rhodamine-B stain afterwards 48 h. Employing AcOH, the extra stain was washed, and applying Tris EDTA buffer, fixed stain was retrieved. Utilizing an ELISA reader, Color Intensity was computed. The drug concentration-surviving portion relevance is plotted for acquiring every cell line survival curvature considering the precise compound. The uninfected and infected response estimates IC_{50} were estimated for the testified compounds (Table 2). As a positive indication, Doxorubicin (DOX) was applied. Compounds stating IC_{50} < 5 µg/mL are contemplated prospectively active and imperilled to extreme *in vivo* considers.

2.4 Telomerase Inhibition Assay

Throughout the published procedure adjustment, the telomeric repeat amplification protocol (TRAP) assay was executed [36]. Applying 10% nondenaturing polyacrylamide gel electrophoresis, the telomerase products were undertaken and were visualized *via* SYBR Green staining (Molecular Probes, USA). Employing LAS-1000 Plus Image analyzer, signal intensity was reckoned (Fuji Film, Japan).

2.5 Preparing and culturing HepG2 2.2.15 cells

Throughout transfecting HepG2 cells with a plasmid encompassing HBV genome (subtype ayw) numerous tandem copies, the needed cell line was accomplished [37]. In RPMI-1640 (Glutamax) culture media holding G418 (geneticin) (380 µg/ml) and nystatin (100 IU/ml), the 2.2.15 cell line was asserted. In a tissue culture hipflask, the relocated HepG2-2.2.15 cell was maintained at 37 ^{o}C + 5% CO_2. Through the cells' cleansing twice with PBS afterward aspirating the culture hipflask media for a week, subcultures were established. For 1 min, throughout incubating the cells, a 10% trypsin/versene was supplemented at 37 ^{o}C. Lamivudine, a selective, potent HBV replication inhibitor, was employed as a gauge.

2.5.1 Extracting DNA

By means of blending diluted supernatant (1:5 with PBS) (ten µl) with 0.2 *M* NaOH (ten µl) inside a reaction tube with incubation for 1 h at 37 ^{o}C, HBV-DNA extraction was performed. Cautiously, 0.2 *M* HCl (9.6 µl) was supplemented subsequently with TE buffer solution (ninety µl).

2.5.2 PCR-Ellisa

In entire volume 50 µl, the PCR reaction mix comprised 4 mmol/l $MgCl_2$, 14 µl extracted supernatant, 10 µmol/l DIG-11-dUTP, 200 µmol/l dATP, 1 µmol/l HCID-1 primer (5′GGA AAG AAG TCA GAA GGC A3′), 190 µmol/l dTTP, dGTP, dCTP, 1.5 U Taq polymerase, 50 mmol/l KCl, 20 mmol/l HCl (pH 8.4), and 1 µmol/l HCID-2 (5′TTG GGG GAG GAG ATT AGG TT3′). For every thermal circler cycle, PCR reaction conditions were 32 cycles at 72 ^{o}C (30 sec), at 58 ^{o}C (30 sec), and at 94 ^{o}C (1 min) + 3 sec [38].

2.5.3 Cytotoxicity Assay

The living cells' colorimetric assay employed 3-(3,5-dimethylthiazol-2-yl)-2,5-diphenyltetrazolium bromide (MTT) as a colorless substratum that is altered through every living cell. Applying MTT assay through culturing the HepG2-2.2.15 cells, the pyrazolo[3,4-*b*]pyridine congeners **1**-**12** cytotoxic influence was retrieved [39].

2.5.4 Calculating IC_{50}, $CC_{50,}$ and SI

Throughout interpolating the DNA copies' amount opposed to antiviral medication concentration plots, the antiviral drugs' 50% inhibitory concentration (IC_{50}) was uncovered. The 50% cytotoxic effect (CC_{50}) was assessed applying the cells' average viability with drug concentration. As CC_{50}/IC_{50}, the selective index (SI) can be assessed [39].

2.6 Docking simulations

Designed for performing molecular docking scores, preparing ligands and the target enzyme, and evaluating ligand-enzyme interaction through visualizing poses and scoring function, Molecular operating environment (MOE: 2019.0102) software was exploited [40, 41]. Employing Protein Data Bank (www.rcsb.org) with PDB id: 2A2B, the target enzyme was regained. The target enzyme was prepared employing the MOE "quick prepare" command, while the ligands were operated by adding protons followed by energy minimization. The docking process was performed employing Forcefield *via* docking placement: Triangular matcher, MMFF94x protocol, refinement: Affinity dG, and Rescoring: London dG.

2.7 Screening ADMET properties

The ADMET profiles, encompassing critical parameters such as cytochrome P450 enzymes inhibition, mutagenicity, Human Intestinal Absorption (HIA), Half-life, Drug-Induced Liver Injury (DILI), carcinogenicity, Skin sensitization, central nervous system (CNS) permeability, and clearance, were evaluated expending ADMETlab 2.0 platform's latest version (July 2021 Release) available at https://admetmesh.scbdd.com/. The platform was fed with the target compound **5**'s SMILES files. The analysis utilized an extensive database with online chemical modeling environment (OCHEM), Toxicity Estimation Software Tools (TEST) established *via* the U.S. Environmental Protection Agency (EPA), DrugBank, PubChem 0.25 million entries, European Molecular Biology Laboratory (ChEMBL) Chemical Database, and peer-reviewed literature [42].

3. Result and Discussion

3.1 Chemistry

A microwave-assisted one-pot multicomponent approach was espoused for simply synthesizing 6,7-dihydro-1*H*-pyrazolo[3,4-*b*]pyridine-5-carbonitrile (**2**) in an excellent yield via conducting a neat mix of 2-methoxybenzaldehyde, ammonium acetate, 5-methyl-2-phenyl-2,4-dihydro-3*H*-pyrazol-3-one, and ethyl cyanoacetate. The reaction may progress by means of imine establishing from ammonium acetate and 5-methyl-2-phenyl-2,4-dihydro-3*H*-pyrazol-3-one, which reacts with ethyl (*E*)-2-cyano-3-(2-methoxyphenyl)acrylate (throughout condensing 2-methoxybenzaldehyde with ethyl cyanoacetate), trailed with cycloaddition, isomerization, and aromatization presenting 4-(2-methoxyphenyl)-3-methyl-6-oxo-1-phenyl-6,7-dihydro-1*H*-pyrazolo[3,4-*b*]pyridine-5-carbonitrile (**2**) (Scheme 1). This reaction is of substantial prominence attributable to its convenient workup, straightforwardly execution, less time consumption, and high yield compared with the conventional two-footstep methodology concerning establishing the chalcone **1** throughout basic Claisen-Schmidt condensation of 5-methyl-2-phenyl-2,4-dihydro-3*H*-pyrazol-3-one with 2-methoxybenzaldehyde tailed with cyclo-condensation with ethyl cyanoacetate and ammonium acetate (Scheme 1).

The chalcone **1** IR spectrum demonstrated the carbonyl group stretching frequency shifting from 1749 cm-1 to 1686 cm^{-1} suggesting the exocyclic double bond formation at the pyrazolone scaffold position-4. The condensation product **1** ^{1}H NMR spectrum recorded a singlet signal at 8.01 ppm corresponding to the *β*-methylene group (CH=C) proton. ^{13}C NMR spectrum affirmed the pyrazolone carbonyl carbon signal at 164.12 ppm, while the *β*-methylene group (CH=C) carbon signal seemed to be at 143.35 ppm. Besides, The pyrazolo[3,4-*b*]pyridine-5-carbonitrile **2** IR spectrum exposed the NH demonstrative band at 3354 cm^{-1} and at 2205 cm^{-1}, a recognizing frequency for the cyano group figured while, the pyridin-2(1*H*)-one ring carbonyl group

frequency looked at 1645 cm^{-1}. ^{1}H NMR exposed a broad singlet signal assigned for the NH group at 11.12 ppm. ^{13}C NMR spectrum markedly championed the pyrazolo[3,4-*b*]pyridine-5-carbonitrile **2** structure posing the CN group signal at 117.08 ppm (*cf.* Scheme 1, experimental section).

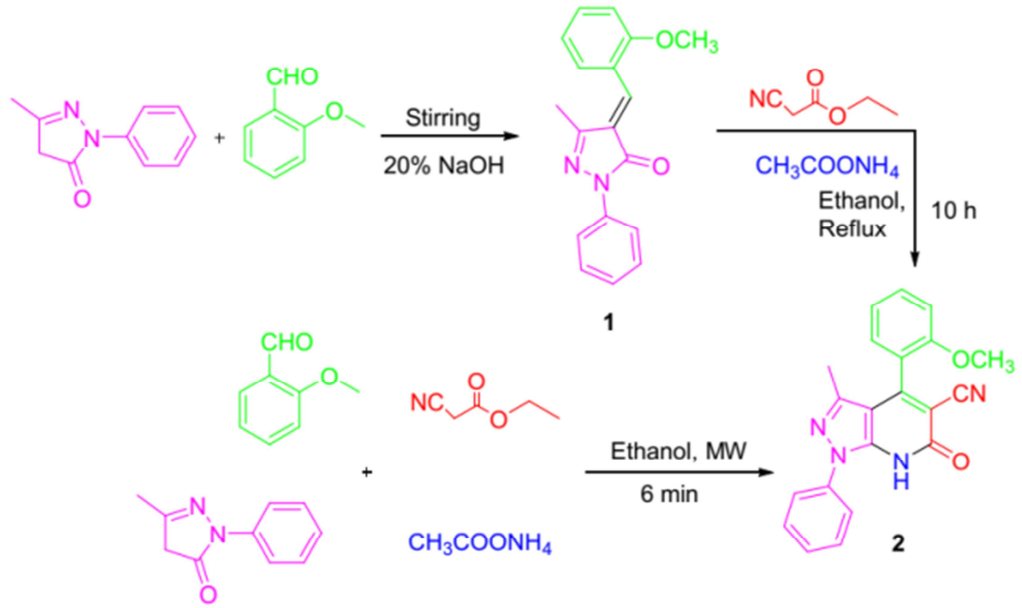

Scheme 1. A synthetic approach to 4-(2-methoxyphenyl)-3-methyl-6-oxo-1-phenyl-6,7-dihydro-1*H*-pyrazolo[3,4-*b*]pyridine-5-carbonitrile (**2**)

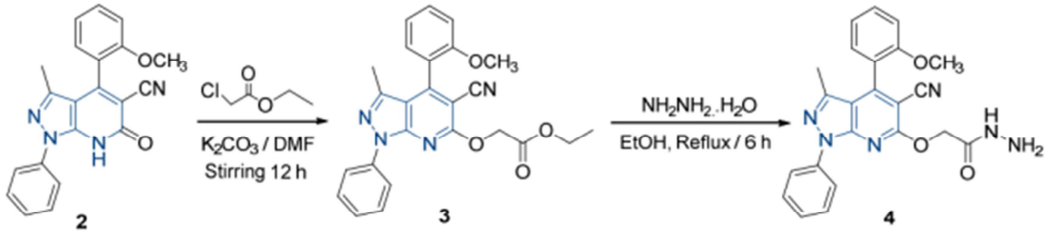

Scheme 2. Synthesis of 1*H*-pyrazolo[3,4-*b*]pyridine-5-carbonitrile derivatives **3** and **4**.

The pyrazolo[3,4-*b*]pyridine-5-carbonitrile **2** was deceptive to be a convenient vital preliminary for generating other novel congeners when treated with ethyl chloroacetate through the nucleophilic substitution reaction (SN^2) employing anhydrous K_2CO_3 engendering the matching *O*-ethyl ester congener **3**. The ester carbonyl group frequency was unveiled in the IR spectrum at 1732 cm^{-1}. The methylene group protons seemed in the ^{1}H NMR spectrum as a singlet signal at 4.62 ppm furnishing a quartet signal for the ester group methylene protons at 4.12-4.16 ppm along with a triplet signal for the ester group methyl protons. ^{13}C NMR spectrum demonstrated the ester group carbonyl carbon signal at 170.05 ppm. Moreover, refluxing the ester **3** with hydrazine hydrate provided the acetohydrazide **4**. At 3132-3319 cm^{-1}, the IR spectrum exhibited the NH_2, NH bands and proved the ester carbonyl group band vanishing. ^{1}H NMR spectrum disclosed the ester

ethyl group protons' non-existence proving the singlet signals attributing to NH_2 and NH groups at 4.31 and 9.87 ppm, correspondingly. ^{13}C NMR spectrum demonstrated the ester group carbonyl carbon and the ethyl group carbons signals disappearance. Compound **4** molecular ion peak was perceived in the anticipated region (*cf.* Scheme 2, experimental section).

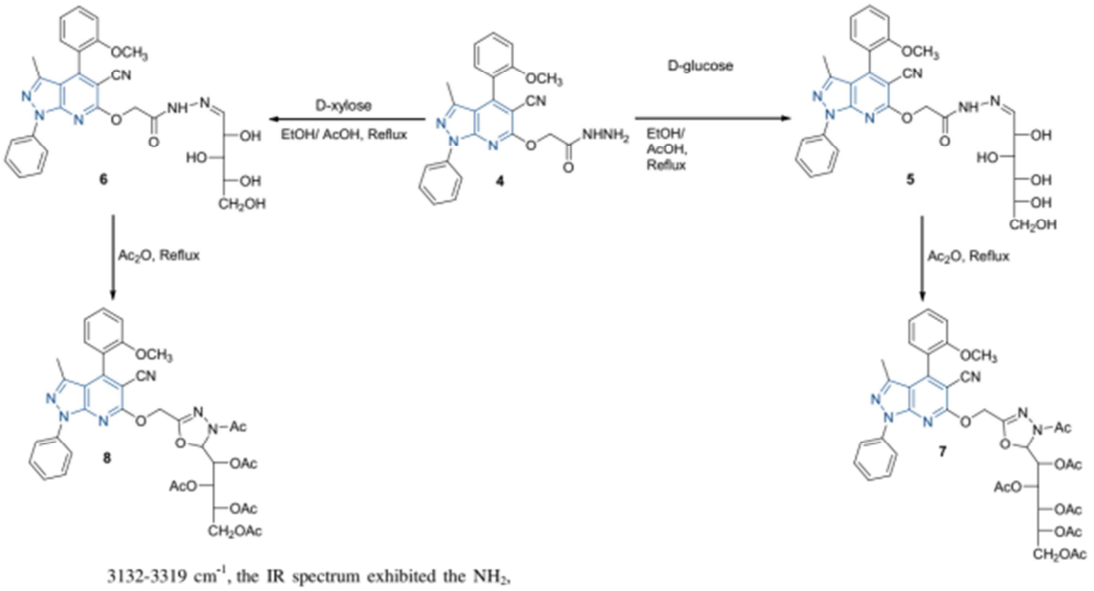

3132-3319 cm^{-1}, the IR spectrum exhibited the NH_2,

Scheme 3. Synthesis of 1*H*-pyrazolo[3,4-*b*]pyridine-5-carbonitrile derivatives **5-8**.

Condensation of D-glucose (**5**) and D-xylose (**6**) with 1*H*-pyrazolo[3,4-*b*]pyridin-6-yl)oxy)acetohydrazide **4** in boiling ethyl alcohol including drops acetic acid presented the sugar hydrazones **5** and **6** with *N*=CH linkage, exemplifying the sugar moieties incorporation in the acyclic *N*-nucleoside system. The produced compounds' structures were established utilizing an assortment of analytical and spectral data. IR spectra exposed the condensed sugar hydroxyl groups' descriptive frequencies in the section 3225–3365 cm^{-1}. ^1H NMR spectra unveiled signals at 3.30–5.65 ppm conveyable to the condensed sugar chain moieties' protons together with the doublet peaks consistent to the condensed sugar moieties (*N*=CH, C^1 methine) protons at 8.20-8.28 ppm along with the aromatic protons' signals. The ^{13}C NMR spectra approved with the anticipated structures exposing new signals attributable to the sugar moieties (*cf.* Scheme 3 and experimental section). $H^{1'}$s high chemical shift value distinguishes the sugar moieties' acyclic form, while in the cyclic form, the sugar moieties' H^1 is stated to seem at lower chemical shift values [41]. Besides, the sugar hydrazones **5** and **6** acetylation, cyclization, and per-*O*-acetylation in boiling acetic anhydride afforded 1,3,4-oxadiazoline acyclic *C*-nucleoside analogs **7** and **8**, correspondingly. The subsequent compounds' structures were founded upon their analytical and spectral data which verified the anticipated structures. Their IR spectra unveiled the carbonyl group frequency at 1738-1739 cm^{-1} and 1630-1631 cm^{-1} consistent with the ester and amide carbonyl groups, correspondingly, representing the *N*-acetyl along with the *O*-acetyl groups incidence. Compounds **7** and **8** ^1H NMR spectra disclosed the *O*-acetyl-methyl protons' signals each as singlet in the extend 1.96-2.06 ppm and the *N*-acetyl group methyl protons at 2.08 ppm. The remaining sugar chain protons existed at 4.09-5.69 ppm incorporating the aromatic protons at 6.76-8.32 ppm. The oxadiazoline ring H^2 ($H^{1'}$ in the prime sugar chain) seemed to be at 6.49 and 6.51 ppm proving its *N,N*-acetal nature more willingly than existing a C=*N*. Over and above, the acetylated hydrazonyl sugar moieties H^1 (already vanished) chemical shift usually looks at higher value

indicating also cyclization had taken place. Compounds **7** and **8** ^{13}C NMR spectra disclosed the amide and ester carbonyl group carbon signals at 170.56-171.92 ppm agreeing with the *N*=CH methine carbon signal vanishing (*cf.* Scheme 3, experimental section).

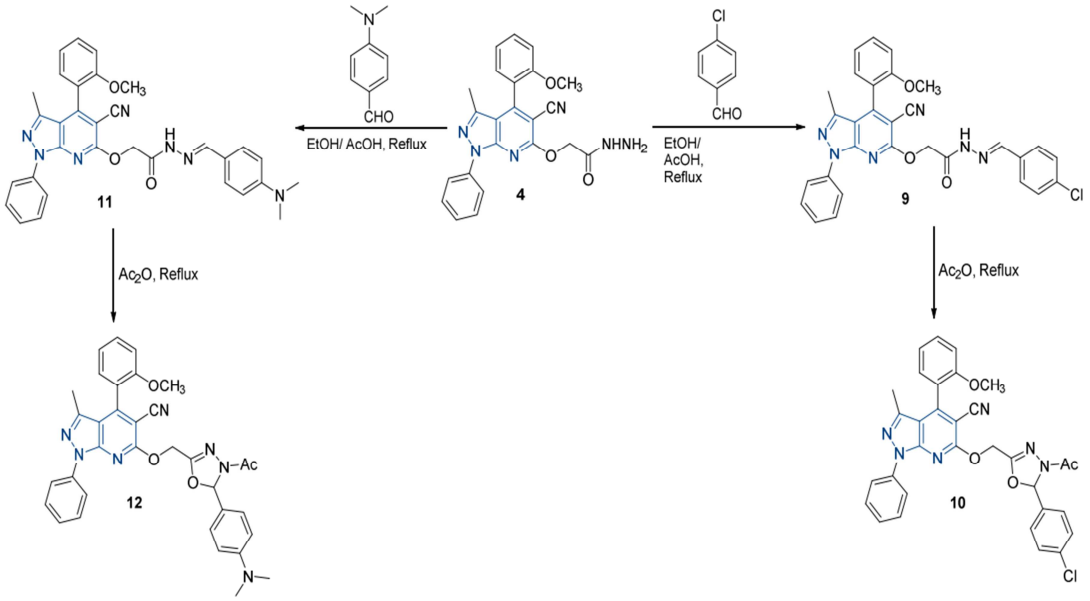

Scheme 4. Synthesis of 1*H*-pyrazolo[3,4-*b*]pyridine-5-carbonitrile derivatives **9-12**.

Furthermore, condensing and refluxing 4-chlorobenzaldehyde and *p*-dimethylaminobenzaldehyde with the 1*H*-pyrazolo[3,4-*b*]pyridin-6-yl)oxy)acetohydrazide **4** in boiling ethyl alcohol containing acetic acid (catalyst) yielded the corresponding Schiff bases **9** and **11**. The IR spectra correspondingly uncovered bands at 3204 and 3213 cm^{-1} regarding NH groups with no absorption frequency in the NH_2 area and correspondingly flourished bands at 1648 and 1649 cm^{-1} for HC=*N* imine groups. ^{1}H NMR spectra exposed a singlet signal at 8.43-8.58 ppm accredited to HC=*N* methine group protons illustrating the non-existence of the NH_2 singlet signal and the NH group existence as broad singlet signals at 11.04 and 11.07 ppm (exchangeable). The ^{13}C NMR spectra provided extreme evidence of the structure (*cf.* Scheme 4, experimental section). Besides, acetylation and cyclization of the Schiff bases **9** and **11** in boiling acetic anhydride afforded 1,3,4-oxadiazoline surrogates **10** and **12**, correspondingly. The subsequent compounds' structures were founded upon their analytical and spectral data which verified the allotted structures. Their IR spectra exhibited amide carbonyl groups' bands at 1655 and 1656 cm-1 representing the incidence of 1,3,4-oxadiazoline *N*-acetyl group. Compounds **10** and **12** ^{1}H NMR spectra disclosed the *N*-acetyl-methyl protons at 2.22 and 2.2 ppm, correspondingly. The oxadiazoline ring H^2 (HC=*N* imine group proton in the Schiff bases) seemed to be at 6.69 and 6.71 ppm proving the cyclization occurrence. Over and above, the Schiff bases' HC=*N* imine group proton (already vanished) chemical shift usually looks at higher value indicating also cyclization had taken place. Compounds **10** and **12** ^{13}C NMR spectra disclosed the amide carbonyl group carbon signals at 169.12 and 169.13 ppm, correspondingly agreeing with the *N*=CH methine carbon signal vanishing (*cf.* Scheme 4, experimental section).

3.2 Antimicrobial assessment

The pyrazolo[3,4-*b*]pyridines **1-12** were assessed in vitro for their antimicrobial efficiencies in contradiction of *Candida albicans* and *Aspergillus flavus* NRRL Y-477 (Fungi), *Bacillus subtilis* NRRL B-543 (Gram +ve bacteria), and *Escherichia coli* NRRL B-210 (Gram -ve bacteria) [43, 44]. The inhibition zone diameters were assessed and contrasted with Penicillin (indication) (Table 1).

The outcomes implied that the 4-(2-methoxyphenyl)-1-phenyl-1*H*-pyrazolo[3,4-*b*]pyridine-5-carbonitril surrogates exposed comparable antimicrobial efficacy with penicillin in opposition to the testified organisms.

Table 1: The pyrazolo[3,4-*b*]pyridine surrogates **1-12** *in vitro* antimicrobial efficacy

Compound	Zone of Inhibition (mm) of Microorganisms			
	Bacillus subtilis	***Escherichia coli***	***Candida albicans***	***Aspergillus flavus***
Penicillin	50 ± 0.24	45 ± 0.12	17 ± 0.26	46 ± 0.27
1	44 ± 0.27	42 ± 0.15	16 ± 0.23	38 ± 0.17
2	49 ± 0.06	45 ± 0.07	14 ± 0.06	39 ± 0.09
3	50 ± 0.13	43 ± 0.09	15 ± 0.05	37 ± 0.05
4	49 ± 0.02	44 ± 0.01	15 ± 0.24	39 ± 0.05
5	49 ± 0.04	46 ± 0.05	17 ± 0.07	45 ± 0.04
6	47 ± 0.08	45 ± 0.07	18 ± 0.18	44 ± 0.02
7	46 ± 0.01	41 ± 0.03	14 ± 0.23	43 ± 0.09
8	47 ± 0.05	43 ± 0.06	15 ± 0.04	46 ± 0.01
9	48 ± 0.08	45 ± 0.07	16 ± 0.02	42 ± 0.04
10	46 ± 0.01	45 ± 0.05	15 ± 0.06	45 ± 0.03
11	45 ± 0.04	44 ± 0.06	16 ± 0.09	45 ± 0.15
12	44 ± 0.05	43 ± 0.07	17 ± 0.12	44 ± 0.23

3.3 Antitumor Assessment

The synthetic compounds **1-12** *in vitro* antitumor efficiency outcomes (Table 2) disclosed an exceedingly momentous upshot contrasted with DOX as an indication versus breast cancer cell line (**MCF-7**).

Table 2: The synthetic compounds' IC_{50} (µg/mL) in opposition to **MCF-7** cell line

Compound	IC_{50} µg/ml
DOX	2.97 ± 0.12
1	4.02 ± 0.04
2	4.50 ± 0.09
3	6.50 ± 0.15
4	5.55 ± 0.23
5	3.01 ± 0.27
6	5.54 ± 0.01
7	4.60 ± 0.06
8	5.15 ± 0.07
9	4.12 ± 0.13
10	3.50 ± 0.09
11	3.01 ± 0.07
12	3.45 ± 0.12

3.4 Telomerase Inhibitory

Telomeres are deemed DNA-protein complexes at the chromosomes terminates, playing a crucial defensive function throughout cell divisions in contradiction of anomalous recombination and DNA degradation [45]. Intended for developing innovative antitumor medications as minor molecules, **I** (IC_{50} = 1.0 µM) was elected as a lead compound established as a telomerase inhibitor throughout Geron. Co. Ltd. (Figure 2) [46, 47].

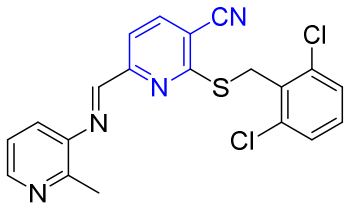

Figure 2. Telomerase Inhibitor, **I**.

The attained outcomes disclosed that pyrazolo[3,4-*b*]pyridines **1-12** were the utmost efficient scaffolds among the telomerase inhibition efficacy testified compounds (IC_{50} 25-44 µM) (Table 3). From the structure activity relationship and the telomerase efficacy outcomes, the attachment of the 4-(2-methoxyphenyl)-1-phenyl-1*H*-pyrazolo[3,4-*b*]pyridine-5-carbonitril congeners exposed higher efficacy.

Table 3: Telomerase inhibition efficiency (IC_{50} (µM)) of the synthetic compounds

Compound	Telomerase Inhibition Efficiency (IC_{50} (µM))
I	1 ± 0.02
1	12 ± 0.04
2	25 ± 0.07
3	27 ± 0.12
4	10 ± 0.06
5	8 ± 0.05
6	9 ± 0.23
7	23 ± 0.04
8	24 ± 0.27
9	29 ± 0.01
10	30 ± 0.15
11	14 ± 0.27
12	28 ± 0.14

3.5 Anti-hepatitis B Assessment

Hepatitis B virus (HBV) is a DNA virus causing acute hepatitis driving to hepatocellular carcinoma, chronic hepatitis, and liver cirrhosis [48]. Every year, over one million fatalities wide-reaching and around 300 million HBV transporters are diseased owing to HBV-associated obstacles [49]. A selective antiviral medication availability versus HBV replication is nonetheless required despite the vaccinations' productive use of HBV infection prevention [50]. Although, various drugs have been assessed, just alpha interferon has established certain clinical value in chosen patients [51, 52].

The HBV life cycle reverse transcription step is the desired intention for antiviral chemotherapy. The progenome reverse transcription is utilized in synthesizing the HBV minus strand applying the endogenous viral reverse transcriptase intended for outperforming cellular DNA polymerase in incorporating nucleotide analogues [53]. The reverse transcriptase viable inhibitors along with the minus strand synthesis cell's cytoplasm nucleosides pool are deemed the nucleotide analogues. The recently developed heterocyclic analogues have exemplified a revolution in discovering selective antiviral efficacies like Lamivudine which operates as a retroviral inhibitor having *in vitro* and *in vivo* efficiency in competition with HBV replication [54].

The investigated compounds' viral screening results versus HBV revealed that **1-12** exhibited modest cytotoxicity with selective indices 166.6 ~ 500.0 and moderate viral replication inhibition.

3.6 Molecular Docking simulation

Compounds **4**, **5**, and **6** were picked as the most potent and effective derivatives versus the telomerase enzyme [PDB id: 2B2A]. This study's preparation and docking steps depended on Molecular operating environment (MOE-2019.0102.) software. The enzyme pockets were studied, and the active site was determined consuming the "Site Finder" command. The resulting outcomes exposed that compound **5** is the most probable effective against telomerase enzyme as it disclosed the finest binding score and interaction pose that comprises two hydrogen bonding (H.B) along with one hydrophobic interaction with the enzyme key amino acid residues Arg A16, Lys B31, and Glu B69, respectively (Figure 3) [55]. Compound **6** exhibited good efficacy against the enzyme inhibitory effect with two hydrogen bond interactions to the key amino acid residues Arg C16 and Lys B31 [55] (Figure 3) and a binding score of -7.1084 kcal/mol. Lastly, compound **4** was of the third rank of the active candidates as it revealed a binding score equal to -6.9100 kcal/mol with hydrogen binding interactions to the enzyme residues Ser B28 and Lys B31 (Figure 3) [55]. It was monitored that the docking outcomes comprising binding interactions and scores were harmonized with the formerly tested IC_{50} values, confirming the docking outcomes (Table 4).

Table4. The target compounds **4**, **5**, and **6** presented interaction and docking simulations versus the telomerase enzyme [PDB id: 2B2A].

Compound	Binding Score (kcal/mol)	Residues	Binding Interactions
4	-6.9100	Ser *B*28	2 H. B
		Lys *B*31	H. B
5	-7.1216	Arg *A*16	H. B
		Lys *B*31	H. B
		Glu *B*69	Hydrophobic interaction
6	-7.1084	Arg *C*16	H. B
		Lys *B*31	H. B

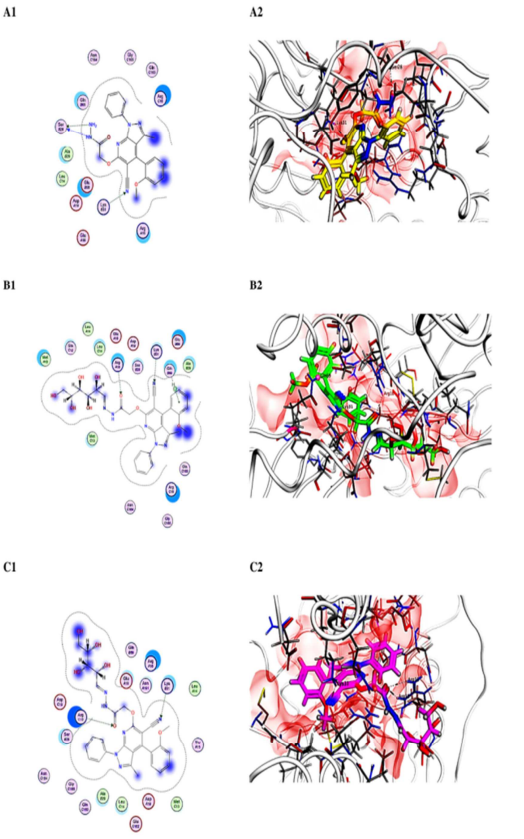

Figure 3. Interaction docking poses for compound **ES4** [A1:2D, A2:3D], compound **ES5** [B1:2D, B2:3D], and compound **ES6** [C1:2D, C2:3D].

3.7 Screening ADMET properties

Assessing compound **5** pharmacokinetic characteristics is crucial for gauging its effectiveness and safety. This investigation scrutinized various factors, involving mutagenicity, Human Intestinal Absorption (HIA), Central Nervous System (CNS) permeability, carcinogenicity, inhibition of Cytochrome P450 enzymes, and drug-induced liver injury. The HIA value is a pivotal determinant affecting bioavailability when processed orally. **5** exhibited positive Human Intestinal Absorption (HIA^+), with an HIA score exceeding 0.1, indicating facile absorption in the human intestine. Conversely, the Blood-Brain Barrier (BBB) permeability index monitors the compound capability in traversing the blood-brain barrier. Compound **5**, upon evaluation, demonstrated an inability in crossing the BBB (BBB score < 0.1, BBB-). Additionally, compound **5** showed no inhibition of cytochrome P450 enzymes (CYP3A4 and CYP1A2). It also displayed high clearance and a short half-life. Furthermore, compound **5** was identified as non-mutagenic, non-blocking the Human ether a-go-go gene (hERG) (hERG score <0.5), non-skin sensitive, and non-carcinogenic. In the screening process, no Bristol-Myers Squibb's (BMS) unsuitable reaction notifies or Pan Assay Interference Compounds (PAINS) were exposed. Consequently, established on these parameters, compound **5** is anticipated to be a secure and dependable compound.

4. Conclusion

The current work designated an effectual facile microwave-supported multi-component procedure for synthesizing 1*H*-pyrazolo[3,4-*b*]pyridine-5-carbonitrile surrogate (**2**) which underwent condensation and cyclization reactions generating novel polyfunctionalized Pyrazolo[3,4-*b*]pyridine congeners **3-12** elucidating their structures by varied spectral means. Fortunately, most of the compounds demonstrated auspicious biological efficiencies. Moreover, in silico study was executed for determining the synthetic Pyrazolo[3,4-*b*]pyridines' expected mode of action. Compounds **4**, **5**, and **6** were picked as the most potent and efficient candidates versus the telomerase enzyme [PDB id: 2B2A]. Besides, compounds **4**, **5**, and **6** were extremely auspicious surrogates in both molecular docking and biological investigations. The conclusions exposed that compound **5** is the extremely plausible efficient alongside the telomerase enzyme due to disclosing the greatest binding score and interaction pose. The synthesized compounds were thought to possess an encouraging ADMET profile. This study presents novel polyfunctionalized Pyrazolo[3,4-*b*]pyridine congeners as favorable accomplishes for proceeding amendment as antimicrobial and antitumor agents. Likewise, compound **5** is worthwhile for extra screening as an eventual chemotherapeutic agent for telomerase inhibition.

5. Conflicts of interest

There are no conflicts to declare.

6. Formatting of funding sources

This research did not receive any specific grant from funding agencies in the public, commercial, or not-for-profit sectors.

7. References

[1] Kim, H. S., Jadhav, J. R., Jung, S. J., Kwak, J. H. (2013). Synthesis and antimicrobial activity of imidazole and pyridine appended cholestane-based conjugates. Bioorganic & medicinal chemistry letters, 23(15), 4315-4318.

[2] El-Assaly, S., Ismail, A. E. H. A., Bary, H., Abouelenein, M. (2021). Synthesis, molecular docking studies, and antimicrobial evaluation of pyrano [2, 3-c] pyrazole derivatives. Current Chemistry Letters, 10(3), 309-328.

[3] Abouelenein, M. G., Ismail, A. E. H. A., Aboelnaga, A., Tantawy, M. A., El-Ebiary, N. M., El-Assaly, S. A. (2023). Synthesis, DFT calculations, In silico studies, and biological evaluation of pyrano [2, 3-c] pyrazole and pyrazolo [4′, 3′: 5, 6] pyrano [2, 3-d] pyrimidine derivatives. Journal of Molecular Structure, 1275, 134587.

[4] Nguyen, H. T., Dang, P. H., Tran, P. H. (2023). A new and straightforward route to synthesize novel pyrazolo [3, 4-b] pyridine-5-carboxylate scaffolds from 1, 4-dihydropyrano [2, 3-c] pyrazole-5-carbonitriles. RSC advances, 13(3), 1877-1882.

[5] Alsoliemy, A. (2023). Synthesis, computational and antimicrobial evaluation of some new pyridine derivatives. Archiv der Pharmazie, 356(3), 2200399.

[6] Abouelenein, M. G., El-Rashedy, A. A., Awad, H. M., El Farargy, A. F., Nassar, I. F., Nassrallah, A. (2023). Synthesis, molecular modeling Insights, and anticancer assessment of novel polyfunctionalized Pyridine congeners. Bioorganic Chemistry, 141, 106910.

[7] Stalinskaya, A. L., Martynenko, N. V., Shulgau, Z. T., Shustov, A. V., Keyer, V. V., Kulakov, I. V. (2022). Synthesis and Antiviral Properties against SARS-CoV-2 of Epoxybenzooxocino [4, 3-b] Pyridine Derivatives. Molecules, 27(12), 3701.

[8] Wang, S., Liu, H., Wang, X., Lei, K., Li, G., Li, X., Quan, Z. (2019). Synthesis and evaluation of anticonvulsant activities of 7-phenyl-4, 5, 6, 7-tetrahydrothieno [3, 2-b] pyridine derivatives. Archiv der Pharmazie, 352(10), 1900106.

[9] Tighadouini, S., Radi, S., Benabbes, R., Youssoufi, M. H., Shityakov, S., El Massaoudi, M., Garcia, Y. (2020). Synthesis, biochemical characterization, and theoretical studies of novel β-keto-enol pyridine and furan derivatives as

potent antifungal agents. ACS omega, 5(28), 17743-17752.
[10] Han, X., Zhou, Q., Wei, J., Tien, P., Yang, G., Wu, S., Dong, C. (2016). A facile one-pot multi-component synthesis of novel adamantine substituted imidazo [1, 2-a] pyridine derivatives: identification and structure–activity relationship study of their anti-HIV-1 activity. RSC advances, 6(97), 95177-95188.
[11] Zhu, S., Tian, X., Liu, J., Dai, B., Li, S. W. Chiral Bipyridine-N, N'-dioxides Catalysts: Design, Synthesis, and Application in Synthesis of 1H-pyrazolo [3, 4-b] pyridine Analogues.
[12] Bhukya, B., Korra, R., Guguloth, H. (2023). Synthesis of novel amide/amino acid functionalized pyrazolo [3, 4-b] pyridine derivatives; their anticancer activity and docking studies. Journal of Heterocyclic Chemistry, 60(5), 872-878.
[13] Labhade, K. R. (2022). Synthesis and Study of Antibacterial Effect of 3, 4-Diaryl-6-oxo-1-phenyl-6, 7-dihydro-1H-pyrazolo [3, 4-b] pyridine-5-carbonitrile. International Journal of Pharmaceutical Investigation, 12(2).
[14] Nassar, I. F.; El Farargy, A. F.; Abdelrazek, F.M. (2018) Synthesis and Anti-Cancer Activity of SomeNew Fused Pyrazoles and Their GlycosideDerivatives J heterocyclic chem., 55, 1709-17719.
[15] Bernardino, A. M. R., de Azevedo, A. R., Pinheiro, L. C. D. S., Borges, J. C., Carvalho, V. L., Miranda, M. D., de Frugulhetti, I. C. P. P. (2007). Synthesis and antiviral activity of new 4-(phenylamino)/4-[(methylpyridin-2-yl) amino]-1-phenyl-1 H-pyrazolo [3, 4-b] pyridine-4-carboxylic acids derivatives. Medicinal Chemistry Research, 16, 352-369.
[16] Samar, C., Ismail, A., Helmi, T., Khiari, J., Bassem, J. (2017). Substituted pyrazolo [3, 4-b] pyridin-3-ones and pyrazolo [3, 4-b] pyridine-5-carbaldehyde, new one-pot synthesis strategy amelioration using vinamidinium salts, antibacterial and antifungal activities promising environmental protection. J. Bacteriol. Parasitol, 8(310), 1-8.
[17] El-Sharkawy, K. A., Ibrahim, R. A. (2013). New approaches for the synthesis and antitumor evaluation of pyridine, thieno [3, 4-c] pyridine, pyrazolo [3, 4-b] pyridine and pyrido [3, 4-d] pyridazine derivatives. Eur. Chem. Bull, 2(8), 530-7.
[18] Figarella, K., Marsiccobetre, S., Galindo-Castro, I., Urdaneta, N., Herrera, J. C., Canudas, N., Galarraga, E. (2018). Antileishmanial and antitrypanosomal activity of synthesized hydrazones, pyrazoles, pyrazolo [1, 5-a]-pyrimidines and pyrazolo [3, 4-b]-pyridine. Current Bioactive Compounds, 14(3), 234-239.
[19] Halder, P., Rai, A., Talukdar, V., Das, P., Lakkaniga, N. R. (2024). Pyrazolopyridine-based kinase inhibitors for anti-cancer targeted therapy. RSC Medicinal Chemistry.
[20] Hawas, S. S., El-Gohary, N. S., Gabr, M. T., Shaaban, M. I., El-Ashmawy, M. B. (2019). Synthesis, molecular docking, antimicrobial, antiquorum-sensing and antiproliferative activities of new series of pyrazolo [3, 4-b] pyridine analogs. Synthetic Communications, 49(19), 2466-2487.
[21] Aggarwal, R., Kumar, S., Sumran, G., Sharma, D. (2024). One-pot synthesis and in vitro bioactivity of novel 4-aminopyrazolo [3, 4-b] pyridine derivatives as potential antimicrobial compounds. Medicinal Chemistry Research, 33(1), 117-126.
[22] Cardoso, C. R., de Brito, F. C., da Silva, K. C., de Miranda, A. L., Fraga, C. A., Barreiro, E. J. (2002). Design, synthesis and pharmacological evaluation of novel pyrazolo [3, 4-b] thieno [2, 3-d] pyridine acid derivatives: a new class of anti-inflammatory and anti-platelet agents. Bioorganic & medicinal chemistry letters, 12(1), 9-12.
[23] Javahershenas, R., Makarem, A., Klika, K. D. (2024). Recent advances in microwave-assisted multicomponent synthesis of spiro heterocycles. RSC advances, 14(8), 5547-5565.
[24] Umar, T., Shalini, S., Raza, M. K., Gusain, S., Kumar, J., Seth, P., Hoda, N. (2019). A multifunctional therapeutic approach: Synthesis, biological evaluation, crystal structure and molecular docking of diversified 1H-pyrazolo [3, 4-b] pyridine derivatives against Alzheimer's disease. European Journal of Medicinal Chemistry, 175, 2-19.
[25] Salem, M. S., Ali, M. A. M. (2016). Novel pyrazolo [3, 4-b] pyridine derivatives: Synthesis, characterization, antimicrobial and antiproliferative profile. Biological and Pharmaceutical Bulletin, 39(4), 473-483.
[26] Menezes, C. M. S., Sant'Anna, C. M. R., Rodrigues, C. R., Barreiro, E. J. (2002). Molecular modeling of novel 1H-pyrazolo [3, 4-b] pyridine derivatives designed as isosters of the antimalarial mefloquine. Journal of Molecular Structure: THEOCHEM, 579(1-3), 31-39.
[27] Cichero, E., Casolino, C., Menozzi, G., Mosti, L., Fossa, P. (2009). Exploring the QSAR of Pyrazolo [3, 4-b] Pyridine, Pyrazolo [3, 4-b] Pyridone and Pyrazolo [3, 4-b] Pyrimidine Derivatives as Antagonists for A1 Adenosine Receptor. QSAR & Combinatorial Science, 28(4), 426-435.
[28] Kurumurthy, C., Veeraswamy, B., Rao, P. S., Kumar, G. S., Rao, P. S., Reddy, V. L., Narsaiah, B. (2014). Synthesis of novel 1, 2, 3-triazole tagged pyrazolo [3, 4-b] pyridine derivatives and their cytotoxic activity. Bioorganic & medicinal chemistry letters, 24(3), 746-749.
[29] Aboelenien, M., Basseem I. Mohamed, M., M. Elsenety, M., A. El-Rashedy, A., H. Ghalib, S., Abdelgalil E. Mohamed, F., A. Ageeli, A. (2024). Facile and Novel Synthetic Approach, Molecular docking, Molecular dynamics, and Drug-Likeness Evaluation of 9-substituted Acridine Congeners as Dual Anticancer and Antimicrobial Agents. Chemistry & Biodiversity, e202301986.
[30] Lourenço, A. L., Salvador, R. R., Silva, L. A., Saito, M. S., Mello, J. F., Cabral, L. M., Sathler, P. C. (2017). Synthesis and mechanistic evaluation of novel N'-benzylidene-carbohydrazide-1H-pyrazolo [3, 4-b] pyridine derivatives as non-anionic antiplatelet agents.

European Journal of Medicinal Chemistry, 135, 213-229.

[31] Marcade, M., Bourdin, J., Loiseau, N., Peillon, H., Rayer, A., Drouin, D., Désiré, L. (2008). Etazolate, a neuroprotective drug linking GABAA receptor pharmacology to amyloid precursor protein processing. Journal of neurochemistry, 106(1), 392-404.

[32] Liu, N., Wang, X., Fu, Q., Qin, Q., Wu, T., Lv, R., Cheng, M. (2023). Design, synthesis and biological evaluation of pyrazolo [3, 4-b] pyridine derivatives as TRK inhibitors. RSC Medicinal Chemistry, 14(1), 85-102.

[33] Tavakoli, E., Sepehrmansourie, H., Zarei, M., Zolfigol, M. A., Khazaei, A., As' Habi, M. A. (2023). Application of Zr-MOFs based copper complex in synthesis of pyrazolo [3, 4-b] pyridine-5-carbonitriles via anomeric-based oxidation. Scientific Reports, 13(1), 9388.

[34] Cruickshank, R., Duguid, J. P., Mormion, B. P., Swain, R. H. A. (1975). Medical Microbiology, 12 th Edn Vol 1 and 2 Churchill Livingstone.

[35] Skehan, P., Storeng, R., Scudiero, D., Monks, A., McMahon, J., Vistica, D., Boyd, M. R. (1990). New colorimetric cytotoxicity assay for anticancer-drug screening. JNCI: Journal of the National Cancer Institute, 82(13), 1107-1112.

[36] Kim, N. W., Piatyszek, M. A., Prowse, K. R., Harley, C. B., West, M. D., Ho, P. L., Shay, J. W. (1994). Specific association of human telomerase activity with immortal cells and cancer. Science, 266(5193), 2011-2015.

[37] Sells, M. A., Zelent, A. Z., Shvartsman, M. A. R. I. N. A., Acs, G. (1988). Replicative intermediates of hepatitis B virus in HepG2 cells that produce infectious virions. Journal of virology, 62(8), 2836-2844.

[38] Korba, B. E., Gerin, J. L. (1992). Use of a standardized cell culture assay to assess activities of nucleoside analogs against hepatitis B virus replication. Antiviral Research, 19(1), 55-70.

[39] Fouad, T., Nielsen, C., Brunn, L., Pederson, E. B. (1998). Use of standardization cell culture assay to assess activities of some potent anti-HIV nucleoside analogues against hepatitis B virus replication. Sc. J. Az. Med. Fac. (GIRLS), 19, 1173-1187.

[40] Said, M. A., Albohy, A., Abdelrahman, M. A., Ibarhim, H. S. (2022). Remdesivir analog as SARS-CoV-2 polymerase inhibitor: virtual screening of a database generated by scaffold replacement. RSC advances, 12(35), 22448-22457.

[41] Allayeh, A. K., El-boghdady, A. H., Said, M. A., Saleh, M. G., Abdel-Aal, M. T., Abouelenein, M. G. (2024). Discovery of Pyrano [2, 3-c] pyrazole Derivatives as Novel Potential Human Coronavirus Inhibitors: Design, Synthesis, In Silico, In Vitro, and ADME Studies. Pharmaceuticals, 17(2), 198.

[42] Xiong, G., Wu, Z., Yi, J., Fu, L., Yang, Z., Hsieh, C., Cao, D. (2021). ADMETlab 2.0: an integrated online platform for accurate and comprehensive predictions of ADMET properties. Nucleic Acids Research, 49(W1), W5-W14.

[43] Su, H. C., Ramkissoon, K., Doolittle, J., Clark, M., Khatun, J., Secrest, A., Giddings, M. C. (2010). The development of ciprofloxacin resistance in Pseudomonas aeruginosa involves multiple response stages and multiple proteins. Antimicrobial agents and chemotherapy, 54(11), 4626-4635.

[44] Rao, H. S. P., Gunasundari, R., Adigopula, L. N., Muthukumaran, J. (2024). Design, synthesis, molecular docking, and biological activity of pyrazolo [3, 4-b] pyridines as promising lead candidates against Mycobacterium tuberculosis. Medicinal Chemistry Research, 33(1), 177-200.

[45] Alanazi, A. F., Parkinson, G. N., Haider, S. (2024). Structural Motifs at the Telomeres and Their Role in Regulatory Pathways. Biochemistry.

[46] Jew, S. S., Park, B. S., Lim, D. Y., Kim, M. G., Chung, I. K., Kim, J. H., Park, H. G. (2003). Synthesis of 6-formyl-pyridine-2-carboxylate derivatives and their telomerase inhibitory activities. Bioorganic & medicinal chemistry letters, 13(4), 609-612.

[47] Mergny, J. L., Mailliet, P., Lavelle, F., Riou, J. F., Laoui, A., Hélène, C. (1999). The development of telomerase inhibitors: the G-quartet approach. Anti-cancer drug design, 14(4), 327-339.

[48] Bousali, M., Papatheodoridis, G., Paraskevis, D., Karamitros, T. (2021). Hepatitis B virus DNA integration, chronic infections and hepatocellular carcinoma. Microorganisms, 9(8), 1787.

[49] Delphin, M., Mohammed, K. S., Downs, L. O., Lumley, S. F., Waddilove, E., Okanda, D., Taljaard, J. (2024). Under-representation of the WHO African region in clinical trials of interventions against hepatitis B virus infection. The Lancet Gastroenterology & Hepatology.

[50] Yardeni, D., Chang, K. M., Ghany, M. G. (2023). Current best practice in hepatitis B management and understanding long-term prospects for cure. Gastroenterology, 164(1), 42-60.

[51] Hristov, A. C., Tejasvi, T., Wilcox, R. A. (2023). Cutaneous T-cell lymphomas: 2023 update on diagnosis, risk-stratification, and management. American journal of hematology, 98(1), 193-209.

[52] Llovet, J. M., Pinyol, R., Yarchoan, M., Singal, A. G., Marron, T. U., Schwartz, M., Finn, R. S. (2024). Adjuvant and neoadjuvant immunotherapies in hepatocellular carcinoma. Nature Reviews Clinical Oncology, 1-18.

[53] Zhao, K., Liu, A., Xia, Y. (2020). Insights into hepatitis B virus DNA integration-55 years after virus discovery. The Innovation, 1(2).

[54] Roy, B., Navarro, V., Peyrottes, S. (2023). Prodrugs of Nucleoside 5'-Monophosphate Analogues: Overview of the Recent Literature Concerning their Synthesis and Applications. Current Medicinal Chemistry, 30(11), 1256-1303.

[55] Sherin, D. R., Manojkumar, T. K., Prakash, R. C., Sobha, V. N. (2021). Molecular docking and dynamics simulation study of telomerase inhibitors as potential anti-cancer agents. Materials Today: Proceedings, 46, 2898-2905.